Understanding the Hydration Structure of Square-Planar Aquaions: The $[Pd(H_2O)_4]^{2+}$ Case

José M. Martínez, Francisco Torrico, Rafael R. Pappalardo, and Enrique Sánchez Marcos*

Departamento de Quimica Fısica, Universidad de Sevilla, 41012-Sevilla, Spain

Received: February 27, 2004; In Final Form: April 26, 2004

Ion solvation of monatomic cations has usually been rationalized on the basis of concentric shell models because of the electrostatic field generated by the metal cation. This work examines, by means of molecular dynamics simulations, the solvation phenomenon for a square-planar hydrate, $[Pd(H_2O)_4]^{2+}$, addressing the question of the structure adopted by water solvent in the regions above and below the molecular plane. Specific ab initio intermolecular potentials describing the interaction between the ion and the solvent have been developed, extending the statistical implementation of the hydrated ion concept. Results show how water molecules in these regions present structural and dynamic properties markedly different from those of the first and the second shells. Whereas average distances are close to those of the first hydration shell, their orientation is similar to that of the second shell, and their mean residence times are even shorter than those of the second hydration shell. This region, called the meso shell, could help in understanding peculiar properties of transition-metal cation square-planar complexes, such as their particular facility to be incorporated in confined regions such as those present in complex biomolecules or interlayered solid structures.

1. Introduction

Despite the large body of knowledge about metal cation solvation, the lack of information concerning the local environment of square-planar ($[Pd(H_2O)_4]^{2+}$ and $[Pt(H_2O)_4]^{2+}$) aquocomplexes is striking.[1−3] There is general agreement on the average structure around octahedral and tetrahedral aquaions; however, the distribution adopted by water molecules surrounding a square-planar hydrate (i.e., the solvent structure in the regions above and below the molecular plane) is not clear. The aim of this work is to supply a picture of this peculiar hydration and its physicochemical implications characterizing the chemistry.

So far, structural determination has mainly focused on the four equatorial water molecules.[4−7] No evidence of axial water molecules has been experimentally observed,[4,8,9] and only Caminiti et al.[10] reports the presence of two axial water molecules in close proximity to the tetrachloro complexes of Pd^{2+} and Pt^{2+} ions by means of X-ray measurements. However, Naidoo et al.[11] by means of molecular dynamics simulations examined the hydration structure around the same chloro complexes, concluding that first hydration shell is composed of eight water molecules occupying the vertexes of a regular tetragonal prism. To the best of our knowledge, only an indirect estimation of the ion neighborhood beyond the first hydration shell has been made by a combined experimental−computational study for the Pt^{2+} case.[8] These studies stress the experimental difficulties in unambiguously determining the presence of axial water molecules coordinating the ion. Two possible situations could be envisaged to understand these findings: a low local density solvent region or a high static and/or dynamic disordered region.

In view of the experimental difficulties involved in attacking this problem, a theoretical approach can offer new insight. A proper treatment must include a subtle balance between the quantum description of the ion−solvent interactions and the intrinsic statistical nature of the solvation phenomenon in the condensed phase.[12−14] In this framework, the combination of first principles interaction potentials with molecular dynamics simulations satisfies the above-mentioned requirements. An appropriate strategy is the use of the hydrated ion model developed by our group to build reliable intermolecular potentials of highly charged metal cations in water solutions. They are based on the assumption that the representative charged species is the hydrated ion $[M(H_2O)_n]^{m+}$. A key point of this approach is based on considering the interaction of water molecules with the cation in the presence of the first hydration shell. Previous implementations of this method were successfully applied to a series of octahedrally and tetrahedrally coordinated cations.[15,16] It is worth pointing out that this first principles quality strategy is a low CPU demanding alternative because of its implementation in classical molecular dynamics simulations.

The square-planar coordination is a much more challenging case because the first hydration shell arrangement does not minimize the water repulsion, being mainly controlled by the electronic properties of the hydrate.[3] The system studied in this work is the Pd^{2+} aquaion for which the mean residence time of the four equatorial water molecules in aqueous solution is $\sim 10^{-3}$ s,[17] 6 orders of magnitude above the typical nanosecond simulation time scale.

2. Methods

2.1. Hydrated Ion Model Potential. The statistical implementation of the hydrated ion model assumes two different types of water molecules, those of the first shell bearing strong nuclear and electronic polarization and partial charge transfer from their direct interaction with the metal cation and those of the bulk solvent. Accordingly, two intermolecular potentials are used to describe the cation−water interactions: IW1 for the first ion−

* Corresponding author. E-mail: sanchez@simulux.us.es.

10.1021/jp049119a CCC: $27.50
Published on Web 07/02/2004

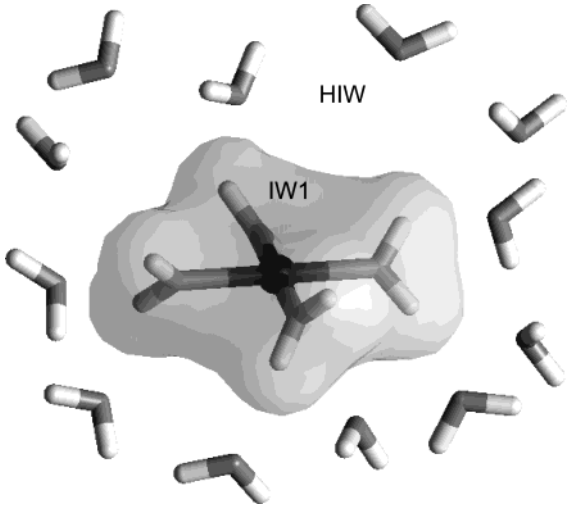

Figure 1. Schematic representation of the hydrated ion approach adopted here, where the IW1 and HIW interaction potential regions are shown.

TABLE 1: Fitted Coefficients for the $IW1_{SP}$ and HIW_{SP} Interaction Potentials[a]

$IW1_{SP}$ potential		HIW_{SP} potential	
coefficient	value	coefficient	value
C_4^{Pd-O}	−11 138.03	D_4^{Pd-O}	3776.71
C_6^{Pd-O}	−29 051.86	D_6^{Pd-O}	−15 669.21
C_8^{Pd-O}	19 864.63	D_{12}^{Pd-O}	−1 023 513.49
C_{12}^{Pd-O}	27 647.40	D_4^{Pd-H}	54.93
C_4^{Pd-H}	0.00	D_6^{Pd-H}	−1222.29
C_6^{Pd-H}	0.00	D_{12}^{Pd-H}	−12 031.29
C_8^{Pd-H}	0.00	D_4^{X-O}	0.00
C_{12}^{Pd-H}	0.00	D_6^{X-O}	12 923.84
C_4^{X-O}	3672.11	D_{12}^{X-O}	259 704.06
C_6^{X-O}	23 619.02	D_4^{X-H}	0.00
C_8^{X-O}	−21 083.63	D_6^{X-H}	865.45
C_{12}^{X-O}	58.25	D_{12}^{X-H}	2907.14
		A_{X-O}	−8466.44
		B_{X-O}	2.05
		A_{X-H}	−100.62
		B_{X-H}	0.96
		r(Pd − X)	0.14

[a] Energies are in kcal/mol, and distances are in angstroms.

water shell[18] and HIW for the hydrated ion−water bulk[19,20] interactions (Figure 1). The internal dynamics of the aquaion is governed by the IW1 potential plus the appropriate water−water interactions.[15,18]

The above-mentioned potentials fit the interaction energies obtained at the MP2 level. For the palladium atom, the pseudopotential of the Stuttgart group (SDD),[21] including relativistic effects, was used, whereas aug-cc-pvdz basis sets for the oxygen and hydrogen atoms were employed.[22] The reference structure for the Pd^{2+} tetrahydrate was constrained to have D_4 symmetry. Two additional interaction sites (termed as X), defining a rigid body with the palladium atom (X−Pd−X), have been placed on the axial direction (above and below the molecular plane) to fulfill two different requirements, absent in all of the previously studied cases where radial symmetry was present: first, the fine tuning of the hydrate−water interactions in the metal exposed regions (axial cone-shaped zones) out of the hydrate molecular plane and second, the need to maintain, on average, a planar structure during the simulation without introducing terms into the interaction potentials higher than two-body contributions such as angular or dihedral ones. To describe the internal dynamics of the tetrahydrate, we defined the interaction energy between the PdX_2 unit and one first-shell water molecule $E_{IW1_{SP}}$ as

$$E_{IW1_{SP}} = \sum_{i}^{PdX\ sites} \frac{C_4^{iO}}{r_{iO}^4} + \frac{C_6^{iO}}{r_{iO}^6} + \frac{C_8^{iO}}{r_{iO}^8} + \frac{C_{12}^{iO}}{r_{iO}^{12}} + \sum_{j}^{water\ sites} \frac{q_{Pd}q_j}{r_{Pd-j}} \quad (1)$$

where the added subscript SP to the IW1 acronym refers to square planar. Seventy interaction energies corresponding to deformations of the reference structure following stretching and bending normal mode patterns were used to fit the corresponding coefficients. Short-range water−water interactions among water molecules belonging to the first hydration shell were computed using the r^{-6} and r^{-12} terms of the TIP4P[23] model potential. Electrostatic charges of Pd, O, and H atoms of the tetrahydrate, 1.31, −0.95, and 0.56 ue, respectively, were obtained by applying the CHELPG method[24] to the solvent polarized[25,26] wave function of the D_4 structure. Table 1 collects IW1 potential parameters.

Hydrated ion−bulk water interactions ($[Pd(H_2O)_4]^{2+}-H_2O$) are considered through the HIW_{SP} potential:

$$E_{HIW_{SP}} = \sum_{i}^{HI\ sites} \sum_{j}^{water\ sites} \frac{D_4^{ij}}{r_{ij}^4} + \frac{D_6^{ij}}{r_{ij}^6} + \frac{D_{12}^{ij}}{r_{ij}^{12}} + \frac{q_iq_j}{r_{ij}} + A_{ij}\cdot e^{B_{ij}r_{ij}} \quad (2)$$

where the exponential term involves only contributions from the X site of the HI unit (i.e., $A_{(Pd-O)} = B_{(Pd-O)} = A_{(Pd-H)} = B_{(Pd-H)} = 0$). Six hundred different arrangements were sampled for the probe water molecule around the hydrate, and the coefficients are also collected in Table 1. Standard deviations of the HIW_{SP} and $IW1_{SP}$ potential fittings are 1.3 and 2.0 kcal/mol, respectively. These values are below 5 and 1% of the representative interaction energies for $[Pd(H_2O)_4]^{2+}-H_2O$ and $[Pd(H_2O)_4]^{2+}$, respectively.

2.2. Molecular Dynamics Simulation Details. Molecular dynamics simulations at 300 K were performed with the MOLDY code[27,28] in the canonical ensemble (*NVT*) using periodic boundary conditions. The simulation cell, containing 1 Pd^{2+} aquaion plus 496 TIP4P[23] water molecules, reproduces a density of 1 g/cm^3. After an appropriate equilibration period, a time step of 2 fs was applied, and atomic positions and velocities were saved every 2 steps for 500 ps for further analysis. Ewald sum methodology[29] was applied to account for the electrostatic interactions, including the charged system term.[30,31]

3. Results and Discussion

3.1. Testing the Potential Behavior by Studying the Hydrate−Water Interaction. Before applying the developed intermolecular potentials in aqueous solution simulations, it is worth examining the interaction of the hydrate and probe water molecules covering the hemispheres above and below the hydrate plane in order to discard spurious effects of the potential. The square-planar nature of the hydrated ion defines a clear asymmetry in the ion−water interaction. In the equatorial region, the interaction is mediated through hydrogen bonds between the first hydration shell and the outer solvent molecules. In this sense, this situation is similar to that found in tetrahedrally and

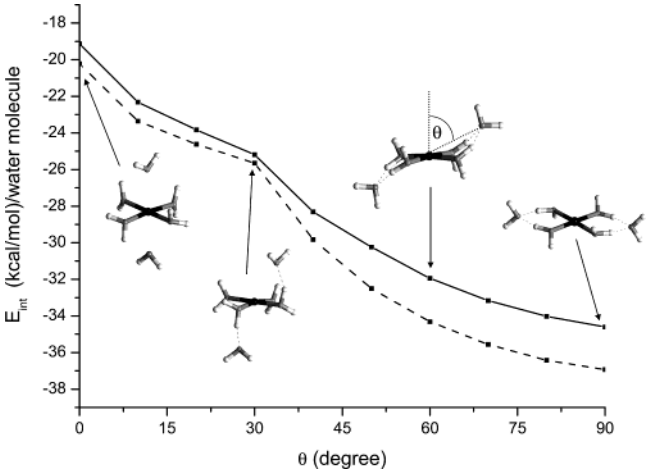

Figure 2. Ab initio (solid line) and HIW_{SP} (dashed line) interaction energy per water molecule between $[Pd(H_2O)_4]^{2+}$ and two water molecules at different θ angles. Some of the computed structures at different θ values are included.

octahedrally hydrated cations. However, in the axial region the interaction is dominated by the direct metal−water interaction.

To perform this test, the interaction between two water molecules and the hydrate have been computed performing a scan that studies the displacement of these water molecules from the axial to the equatorial region. The only geometrical constraints imposed are the azimuthal angle defining the relative position of the probe water molecules against the molecular plane of the hydrate and the internal geometry of the water molecules. To retain the geometrical equivalence of the two hemispheres, one water molecule on each side has been taken into account. To reduce computational costs, the geometrical optimizations have been performed at the B3LYP level, albeit the interaction energy is computed at the same level as that used in the potential development (i.e., the MP2 level). In Figure 2, the ab initio interaction energies can be compared with the HIW_{SP} energies. The developed potential follows the quantum mechanical energy profile along the angular coordinate fairly well. The main difference is found for the equatorial region, where a double hydrogen bond is observed. At this point, one has to take into account that this situation is highly unlikely in the condensed medium and therefore was not considered in the potential development. However, this overall reasonable agreement (∼1 kcal/mol) illustrates the good behavior of the HIW_{SP} potential.

3.2. Molecular Dynamics Results. The general behavior of the developed intermolecular potentials has been tested by estimating a set of properties of the ionic solution, such as the cation hydration enthalpy, ion mobility, or structural and dynamic characterization of the ion environment.

The estimated hydration enthalpy for Pd^{2+} is -547 ± 45 kcal/mol, to be compared with the experimental value of −491 kcal/mol.[32] The main contribution of many-body effects present in close proximity to the ion has been clearly taken into account through the hydrated ion methodology. The 10% overestimation comes from the lack of a polarizable solvent model that largely corrects, as previously shown,[33] the remaining many-body effects in the second hydration shell region.

The translational self-diffusion coefficient of Pd^{2+} has been obtained both from the ion velocity autocorrelation function and from the mean-square displacement. The computed value, $(0.67 \pm 0.05) \times 10^{-5}$ cm^2/s, is in good agreement with the most recent experimental determination of this magnitude, 0.83×10^{-5} cm^2/s, given by Uemoto in 2000,[34] and is quite different from the previously reported value, 1.99×10^{-5} cm^2/s, in Marcus' compilation.[32]

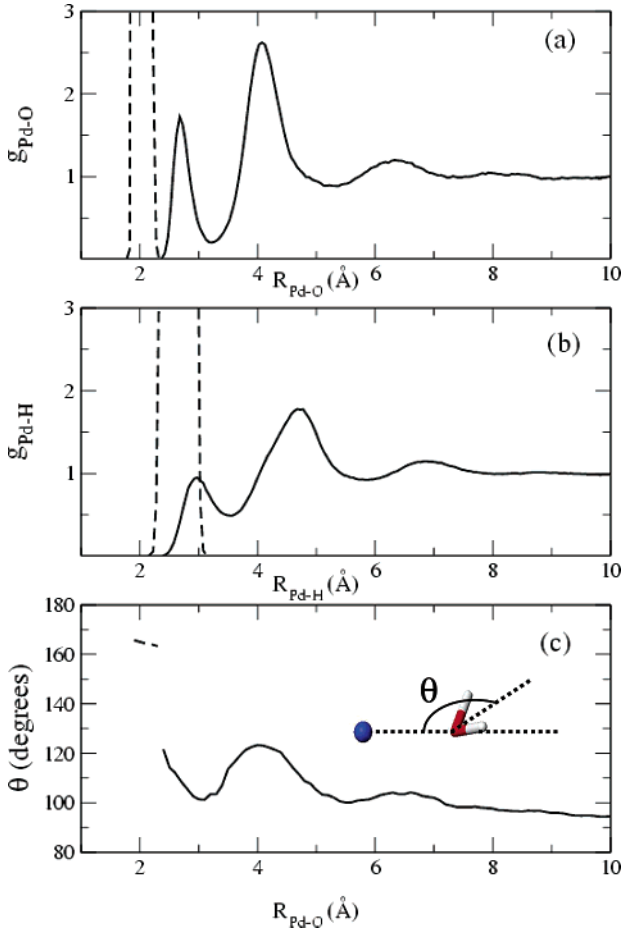

Figure 3. Pd−O (a) and Pd−H (b) radial distribution functions and the orientational parameter (θ) as a function of the Pd−O distance (c). Dashed lines represent first-shell water molecules, and solid lines represent bulk water.

3.2.1. Defining the Hydration Structure around Pd^{2+}: The Meso-Shell Concept. Pd−O radial distribution functions plotted in Figure 3a show three well-defined peaks. The first and the third ones, centered at 2.00 and 4.08 Å, respectively, correspond to the first- and second-shell water molecules and integrate to 4 and 16 solvent molecules, respectively. The middle peak appearing at 2.67 Å integrates to two water molecules. These results contrast sharply with those of the more usual tetrahedral or octahedral hydrates (Li^+, Be^{2+}, Al^{3+}, Cr^{3+}), where only two well-defined peaks for the first and second hydration spheres are found.[1,15] The analysis of the Pd−H radial distribution function (Figure 3b) reinforces the appearance of the intermediate shell at 2.98 Å that is partially overlapped by the first Pd−H peak, centered at 2.68 Å, corresponding to the eight hydrogen atoms of the first hydration shell. Both Pd−O and Pd−H RDFs support the presence of two axial water molecules. According to the previous examination of the interaction energy derived either from ab initio or from the newly developed potential, there is no minimum in the axial region, and only a smooth transition from this region is observed to the more stabilizing equatorial situation. Then, the origin of this peak in the RDFs is clearly a cooperative effect of the condensed medium, where specific interactions and steric effects are taken into account.

It is worth pointing out that these axial molecules are not oriented following the usual charge−dipole pattern in view of the maximum positions of the middle peak in both distributions

(2.67 Å for Pd−O versus 2.98 Å for Pd−H). This fact is quantified by the orientational parameter plotted in Figure 3c. The tilt angle drops from 165° for the first-shell water molecules to 110° for the axial water molecules and increases again to 122° for the second-shell solvent molecules hydrogen bonded to the equatorial first shell. This structural arrangement points out how the second-sphere equatorial water molecules are more oriented toward the ion than the axial water molecules are. This finding reflects a new structural pattern where there is not a simple relationship between water orientation and distance to the cation.

An additional property, useful for the understanding of the hydration phenomenon, is related to the persistence of the solvent molecules in close proximity to the ion. The mean residence times[35,36] of water molecules in the axial and second-sphere regions are 4 ± 1 and 12 ± 1 ps, respectively.[37] This dynamic behavior reflects other specific features of the water molecules located in the axial region: a molecule ca. 2.7 Å from the ion is less tightly bonded to the cation than the water molecules coordinated to the equatorial first shell at ca. 4.1 Å. This result also shows a new dynamic pattern for the axial water region, where the persistence of the solvent in the different coordinating regions is not a monotonic function of the cation−solvent distance.

The identification of important solvent binding sites can be visualized by means of spatial distribution functions (SDFs)[38] of solvent atoms around the metal ion. This 3-D picture, defined by isovalue surfaces, shows the highest probability regions for finding a given type of atom in the neighborhood of the ion. Figure 4 shows the axial and equatorial views of the SDFs corresponding to the first-shell hydrogen atoms and the oxygen atoms of the bulk solvent, represented by surfaces enclosing 25% of the total probability. For instance, the narrow yellow surfaces, corresponding to the first-shell hydrogen atoms, show the low probability of finding the equatorial water molecules with the hydrogen atoms perpendicular to the $[Pd(H_2O)_4]^{2+}$ molecular plane, a clear indication of highly restricted librational motions. Oxygen atoms of bulk water molecules can be located in two nonoverlapping regions differently colored in Figure 4. The well-defined green lobes of the SDF belong to the water molecules interacting with the equatorial first shell and also reflect the above-mentioned hydrogen distribution that they are bonded to. The blue SDF clearly corresponds to the axial water molecules, previously identified in the Pd−O RDF.

Two features must be recognized in the nonequatorial regions. First, the wide blue region that a single molecule covers implies that a low local density must be found above and below the square-planar hydrate. Second, the presence of nonnegligible probability zones, is indicated green spots not included in the green lobes, at distances corresponding to the second hydration shell according to the Pd−O RDF. The water molecules contributing to these green spots play a bridging role between the axial and the second-shell water molecules,[39] remaining in these bridging regions for very short periods (mean residence time ∼1 ps). A typical arrangement of the above-mentioned water molecules in close proximity to the cation can be observed in Figure 5.

When Frank and Evans[40] proposed their model of concentric solvation shells in the 1940s, they were summarizing in an extremely powerful and simple way the quite general behavior of single ions generating a roughly spherical interaction field around them. However, in some cases, the electronic properties of metal ions determine coordination environments, particularly in biochemical structures,[41] ruled by nonradial patterns. The

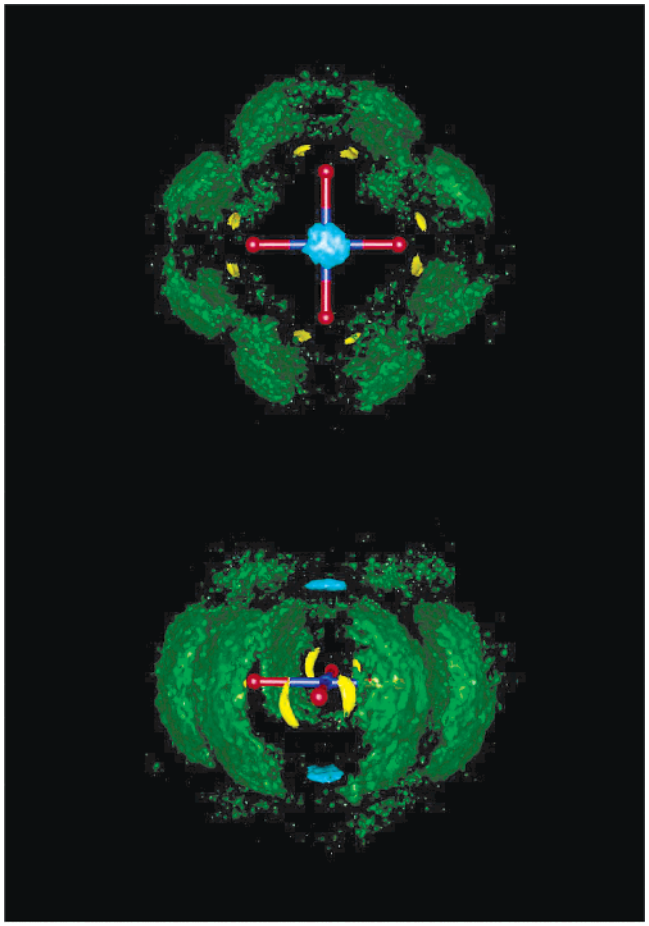

Figure 4. Spatial distribution functions (SDFs) around Pd^{2+} for first-shell hydrogen atoms (yellow) and bulk water oxygens (blue for axial water molecules and green for the second shell and bridging solvent molecules). For clarity, SDFs corresponding to bulk solvent hydrogen atoms are not shown. Axial view (top) and equatorial view (bottom).

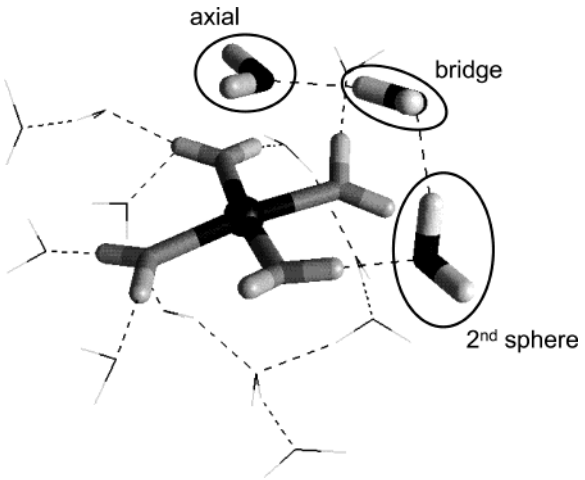

Figure 5. Snapshot of the MD simulation showing a typical arrangement for axial and second-shell water molecules linked by a bridging molecule.

proper understanding of the hydration of square-planar hydrated ions needs the introduction of a new concept tightly joined to the observed facts taking place above and below the molecular plane. Water molecules in these regions present structural and dynamical properties between those characterizing the classical definition of the first and second hydration shells. This intermediate shell is located at distances close to those of a first hydration shell, but its characteristic residence time corresponds

to that of a loosely bonded second hydration shell. The term meso shell can be proposed to identify water molecules behaving in such a way. This characterization emphasizes the fact that a strong asymmetry of the hydration is present in the environment closest to this cation. A direct consequence of this study is the better understanding of the experimental results concerning the structural characterization in solution of the square-planar ions. Time-dependent properties can explain the difficulties associated with the experimental detection of axial water molecules,[4,8−10] despite their clear contribution to the RDF obtained from the MD simulations.

4. Concluding Remarks

The question addressed at the beginning of this work concerning the solvent structure around the Pd^{2+} ion has been answered by the introduction of the meso shell where no preferential binding sites are found, despite being an attractive region for the ion−water interaction. Its structural and dynamical properties come from the combination of the above-mentioned feature with the condensed-medium effects. In this sense, the meso shell is characterized by a well-defined peak in the metal−oxygen RDF, a low local density in the corresponding SDF, and residence times lower than those of the second hydration shell. Therefore, the experimental difficulties associated with its identification must be understood on the basis of the last two facts.

The approach presented here can be easily extended not only to square-planar aquaions but also to other square-planar complexes for metal ions such as Cu^{2+} or Pt^{2+} involving, for instance, N-coordinating ligands.[41,42] In this sense, the methodology proposed fairly describes the different nature of the ion−solvent interactions observed for the solvent molecules directly interacting with the metal ion (i.e., those coordinating the planar and axial positions and characterized by residence times differing by several orders of magnitude). In fact, the identification of the meso-shell region can be crucial for understanding the solution chemistry of these ions, involved in relevant processes and not observed for structures lacking planarity, such as the intercalation mechanisms of square-planar aggregates in complex biochemical structures. In this sense, the meso shell presents peculiarities that make it very different from the first or the second hydration shell: it covers a large region of the immediate vicinity of the ion with a small number of solvent molecules that additionally favor an easy dehydration of this zone.

We believe that the new concept of the meso shell, shown by the methodology presented here for square-planar complexes, can open new approaches in the field of the solution chemistry of these systems.

Acknowledgment. Fundación Ramón Areces is acknowledged for financial support. We thank Professors J. Bertrán, I. Grenthe, and F. Sánchez Burgos for making useful comments.

References and Notes

(1) Ohtaki, H.; Radnai, T. *Chem. Rev.* **1993**, *93*, 1157−1204.
(2) Marcus, Y. *Ion Solvation*; Wiley: Chichester, U.K., 1986.
(3) Richens, D. T. *The Chemistry of Aqua Ions*; John Wiley: Chichester, U.K., 1997.
(4) Hellquist, B.; Bengtsson, L.; Holmberg, B.; Hedman, B.; Persson, I.; Elding, L. I. *Acta Chem. Scand.* **1991**, *45*, 449−455.
(5) Deeth, R. J.; Elding, L. *Inorg. Chem.* **1996**, *35*, 5019−5026.
(6) Zeizinger, M.; Burda, J. V.; Sponer, J.; Kapsa, V.; Leszcynski, J. *J. Phys. Chem. A* **2001**, *105*, 8086−8092.
(7) Burda, J. V.; Zeizinger, M.; Sponer, J.; Leszcynski, J. *J. Chem. Phys.* **2000**, *113*, 2224−2232.
(8) Ayala, R.; Sánchez Marcos, E.; Díaz-Moreno, S.; Solé, V. A.; Muñoz Páez, A. *J. Phys. Chem. B* **2001**, *105*, 7588−7593.
(9) Gröning, O.; Drakenberg, T.; Elding, L. I. *Inorg. Chem.* **1982**, *21*, 1820−1824.
(10) Caminiti, R.; Carbone, M.; Sadun, C. *J. Mol. Liq.* **1998**, *75*, 149−158.
(11) Naidoo, K.; Klatt, G.; Koch, K.; Robinson, D. *Inorg. Chem.* **2002**, *41*, 1845−1849.
(12) Pasquarello, A.; Petri, I.; Salmon, P. S.; Parisel, O.; Car, R.; Toth, E.; Powell, D. H.; Fischer, H. E.; Helm, L.; Merback, A. E. *Science* **2001**, *291*, 856−859.
(13) Tuckerman, M. E.; Marx, D.; Klein, M. L.; Parrinello, M. *Science* **1997**, *275*, 817−820.
(14) Tuckerman, M. E.; Marx, D.; Parrinello, M. *Nature (London)* **2002**, *417*, 925−929.
(15) Martínez, J. M.; Pappalardo, R. R.; Sánchez Marcos, E. *J. Am. Chem. Soc.* **1999**, *121*, 3175−3184.
(16) Merkling, P.; Muñoz Páez, A.; Sánchez Marcos, E. *J. Am. Chem. Soc.* **2002**, *124*, 10911−10920.
(17) Helm, L.; Merbach, A. E. *Coord. Chem. Rev.* **1999**, *187*, 151−181.
(18) Martínez, J. M.; Pappalardo, R. R.; Sánchez Marcos, E. *J. Chem. Phys.* **1998**, *109*, 1445−1455.
(19) Pappalardo, R. R.; Sánchez Marcos, E. *J. Phys. Chem.* **1993**, *97*, 4500−4504.
(20) Pappalardo, R. R.; Martínez, J. M.; Sánchez Marcos, E. *J. Phys. Chem.* **1996**, *100*, 11748−11754.
(21) Andrae, D.; Haeussermann, U.; Dolg, M.; Stoll, H.; Preuss, H. *Theor. Chim. Acta* **1990**, *77*, 123−141.
(22) Woon, D.; Dunning, T. H. J. *J. Chem. Phys.* **1993**, *98*, 1358−1371.
(23) Jorgensen, W. L.; Chandrasekhar, J.; Madura, J. D.; Impey, R. W.; Klein, M. L. *J. Chem. Phys.* **1983**, *79*, 926−935.
(24) Breneman, C. M.; Wiber, K. B. *J. Comput. Chem.* **1990**, *11*, 361−373.
(25) Miertus, S.; Scrocco, E.; Tomasi, J. *Chem. Phys.* **1981**, *55*, 117.
(26) Mennucci, B.; Cancès, E.; Tomasi, J. *J. Phys. Chem. B* **1997**, *101*, 10506.
(27) Refson, K. *MOLDY User's Manual*, rev. 2.10. MOLDY code can be obtained from the CCP5 program library.
(28) Refson, K. *Comput. Phys. Commun.* **2000**, *126*, 310−329.
(29) Allen, M. P.; Tildesley, D. J. *Computer Simulation of Liquids*; Oxford University Press: Oxford, U.K., 1987.
(30) Leslie, M.; Gillan, M. *J. Phys. C: Solid State Phys.* **1985**, *18*, 973−982.
(31) Roberts, J. E.; Schnitker, J. *J. Phys. Chem.* **1995**, *99*, 1322−1331.
(32) Marcus, Y. *Ion Properties*; Marcel Dekker: New York, 1997.
(33) Martínez, J. M.; Hernández-Cobos, J.; Saint-Martin, H.; Pappalardo, R.; Ortega-Blake, I.; Sánchez Marcos, E. *J. Chem. Phys.* **2000**, *112*, 2339−2347.
(34) Uemoto, M. *Inorg. React. Mech.* **2000**, *2*, 155−159.
(35) Impey, R. W.; Madden, P. A.; McDonald, I. R. *J. Phys. Chem.* **1983**, *87*, 5071−5083.
(36) Garcia, A. E.; Stiller, L. *J. Comput. Chem.* **1993**, *14*, 1396−1406.
(37) Mean residence times were computed with $t^* = 0$ ps, t^* representing the maximum allowed time a solvent molecule can leave a specific region without loosing its ascription. Usually, in water simulations, $t^* = 2$ ps is also common. In this case, 10 and 19 ps are obtained for the mean residence times of axial and second-shell water molecules.
(38) Kusalik, P. G.; Laaksonen, A.; Svishchev, I. M. In *Molecular Dynamics: From Classical to Quantum Methods*; Elsevier: Amsterdam, 1999; Chapter 3.
(39) Stace, A. *Science* **2001**, *294*, 1292−1293.
(40) Frank, H. S.; Evans, M. W. *J. Chem. Phys.* **1945**, *13*, 507−532.
(41) Lippard, S. J.; Berg, J. M. *Principles of Bioinorganic Chemistry*; University Science Books: Mill Valley, CA, 1994.
(42) Burda, J. V.; Sponer, J.; Leszcynski, J. *Phys. Chem. Chem. Phys.* **2001**, *3*, 4404−4411.